

G. Gruner

## Carbon nanotube transistors for biosensing applications

Received: 4 April 2005 / Revised: 13 June 2005 / Accepted: 15 June 2005 / Published online: 30 August 2005  
© Springer-Verlag 2005

**Abstract** Electronic detection of biomolecules, although still in its early stages, is gradually emerging as an effective alternative to optical detection methods. We describe field effect transistor devices with carbon nanotube conducting channels that have been developed and used for biosensing and biodetection. Both transistors with single carbon nanotube conducting channels and devices with nanotube network conducting channels have been fabricated and their electronic characteristics examined. The devices readily respond to changes in the environment, and such effects have been examined using gas molecules and coatings with specific properties. Device operation in (conducting) buffer and in a dry environment—after buffer removal—is also discussed. Applications in the biosensing area are illustrated with three examples: the investigation of the interaction between devices and biomolecules, the electronic monitoring of biomolecular processes, and attempts to integrate cell membranes with active electronic devices.

**Keywords** Carbon nanotube transistor · Nanoscale devices · Electronic detection · Bioelectronic integration · Celectronics

### Introduction

Most biological sensing techniques rely largely on optical detection principles. These techniques are highly sensitive and specific but are inherently complex, for

they involve multiple steps between the actual engagement of the analyte and the generation of a signal. These techniques require multiple reagents, preparative steps, signal amplification, and complex data analysis. Single molecule detection, while demonstrated in a few cases, requires the application of optical probe molecules that may change the functionality of the biomolecules in question. Electronic detection, utilizing nanoscale devices, offers advantages for two reasons. The first is size compatibility. Thanks to recent advances in nanoscale materials, we are now able to construct electronic circuits in which the component parts are comparable in size to biological entities, thus ensuring appropriate size compatibility between the detector and the detected species. Some length scales in Fig. 1 illustrate this observation: single cells are approximately 1  $\mu\text{m}$  in size; viruses are approximately 100 nm; individual proteins are on the order of 10 nm; and the diameter of the DNA duplex is approximately 1 nm. Compare this with the size range for nanostructures: optical lithography-based nanowire fabrication reaches down to 100 nm, the size of a typical virus. E-beam fabrication has a current limit of approximately 30 nm, and innovative printing technologies also reach this length scale. The typical cross-section of fabricated semiconductor nanowires is currently on the order of 10 $\times$ 10 nm, the approximate size of a protein. The diameter of single-wall carbon nanotubes—naturally occurring hollow cylinders—is in the 1 nm range, the diameter of the DNA duplex. The second advantage to developing electronic detection schemes is that most biological processes involve electrostatic interactions and charge transfer, which allows electronic detection and the eventual merging of biology and electronics.

Because of the rich potential of biosensors [1] and bioelectronics [2], recent research has focused on the interactions between biomolecules and inorganic systems. The integration of biological processes and molecules with fabricated structures also offers both electronic control and sensing of biological systems and

G. Gruner  
Department of Physics, University of California Los Angeles,  
Los Angeles, CA 90095, USA  
E-mail: ggruner@ucla.edu

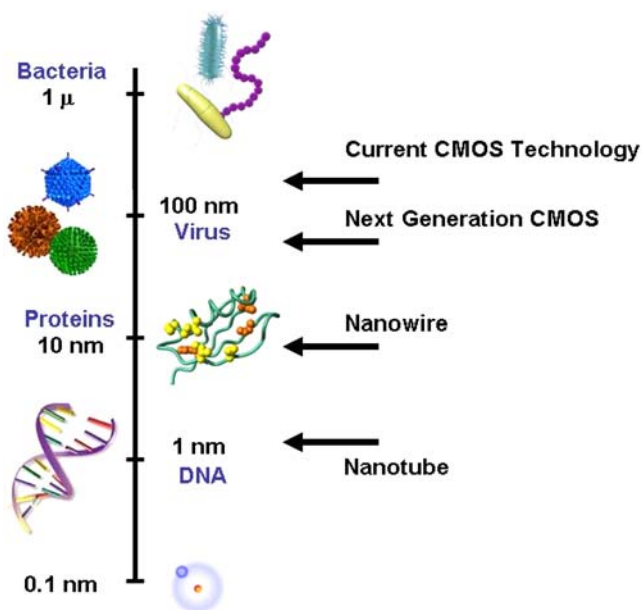


**Fig. 1** The dimensions of wires used in conventional CMOS technology, together with as-grown nanowires and carbon nanotubes. While the cross-section of nanofibers and inorganic nanowires is comparable to the size of typical proteins, single wall carbon nanotubes (hollow cylinders of carbon) have a diameter comparable to DNA

bioelectronically-driven nanoassembly [3]. As a specific example, carbon nanotubes (hollow cylinders made of sheets of carbon atoms) have been suggested for use as prosthetic implants in nervous systems [4], and this goal requires the integration of fully-functioning biological and nanoelectronic systems. Thus far, researchers have used organic and inorganic chemistry to attach proteins [5], DNA [6], and lipids [7] to nanotubes, nanowires, and nanocrystals. In such bottom-up construction, a single biological species is integrated with a single type of nanostructure, usually in solution. To move towards functional devices, further processing is required, which may damage the biological molecules. However, forming more complex biological structures requires that biological activity be preserved despite the presence of the nanostructures. As a result, the nanostructures have served only as mechanical support (for example as substrates), without electronic functionality [2].

Transistors, the fundamental elements of active electronics, are the natural link that can be used for the purpose described above, and one can also use various characteristics of a transistor to gain detailed information on the biological processes that take place. Conventional transistors have been used extensively [8–11]; these, however, do not have the inherent sensitivity that would make them comparable to certain optical techniques. Transistors that incorporate molecular nanowires [12–14] have also been used for the detection of DNA, proteins and viruses, and they remain a viable technology worth exploring.

Carbon nanotubes have recently also emerged as building blocks of novel nanoscale structures and devices [15]. Nanotubes can be viewed as a rolled-up sheet of graphite—a sheet formed of hexagons of carbon atoms. Depending on the detailed geometry, nanotubes have a variety of electronic properties that can be exploited for a variety of applications. Nanotubes have been functionalized to be biocompatible and to be capable of recognizing proteins [16–19]. Often this functionalization has involved noncovalent binding between a bifunctional molecule and a nanotube in order to anchor a bioreceptor molecule with a high degree of control and specificity. The unique geometry of nanotubes has also been used to modify nanotube-protein binding. The conformational compatibility, driven both by steric and hydrophobic effects, between proteins and carbon nanotubes has been examined using streptavidin and other proteins. For example, streptavidin has been crystallized in a helical conformation around multi-walled carbon nanotubes [20]<sup>1</sup>. Conversely, the tendency of biological materials to self-organize has been used to direct the assembly of nanotube structures [21].

Devices built of carbon nanotubes offer several advantages for the detection of biological species. First, nanotubes form the conducting channel in a transistor configuration, the most essential part of the architecture. Second, the nanotubes, typically located on the surface of the supporting substrate, are in direct contact with the environment. In contrast, for conventional CMOS-fabricated transistors, the conducting channel (the so-called depletion layer) is buried in the material in which the depletion layer is formed. Third, all of the current flows at the surface of the tubes. All these attributes lead to a device configuration that is extremely sensitive to minute variations in the surrounding environment.

Field effect transistors (FETs) fabricated using semiconducting single-wall carbon nanotubes (SWNTs) as the conducting channel (nanotube FETs and NTFETs) have been studied extensively [22, 23], and the electronic characteristics of the devices have been thoroughly explored and are reasonably well understood. The devices have been found to be sensitive to various gases [24, 25], such as ammonia, and thus can operate as sensitive chemical sensors. In our work [26, 27], and that of some other groups [28], the electronic detection of chemical species in a liquid environment has been explored. We have also found that these devices are extremely sensitive, and are able to detect a single molecule both in air and in a (conducting and non-conducting) liquid environment. Such devices are also promising candidates for electronic detection of

<sup>1</sup>Comment on 20, Balavoine et al (1999) *Angew Chem Int Edit* 38:1912 (*Helical crystallization of proteins on carbon nanotubes: a first step towards the development of new biosensors*): Of course, proteins are easily immobilized on other surfaces, including the silicon substrate onto which the nanotube conducting channels are deposited. The presence of biomolecules on a surface that does not participate in the conduction process will, however, not influence the device's characteristics.

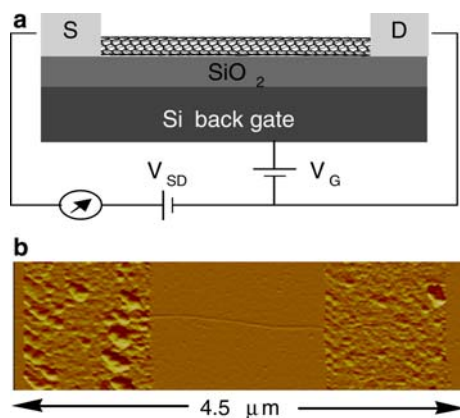


**Fig. 2a–b** Field effect transistor with carbon nanotube conducting channel. *S* and *D* refer to the source and drain. **a** Schematic of a single nanotube channel transistor (*NTFET*) in a so-called back-gate configuration. **b** AFM image of a *NTFET* device. The thin horizontal line is the nanotube connecting the source and drain electrodes

biological species. Initial studies described in [29–31]<sup>2</sup> indicate that the extreme sensitivity of the devices may—after improvement of the device characteristics, such as noise, and in an appropriately fabricated environment—lead to single biomolecule detection and to real-time monitoring of conformational changes of biomolecules.

## Device architectures

Two different device architectures, both utilizing carbon nanotubes that connect the source and drain electrodes, have been developed and explored by various groups working in this area. In one device architecture, a single nanotube connects the source and the drain, in a configuration that is shown in Fig. 2. Such devices have been utilized for biosensing, and they offer excellent sensitivity. There is, however, substantial variation between the different devices that are fabricated. Such variation reflects the (geometry-dependent) variation in the electronic characteristics of individual nanotubes. In addition, the interface between the nanotube and the

<sup>2</sup>Comment on 29, Bradley et al (2004) *Nano Lett* 4:253 (*Charge transfer from adsorbed proteins*): The number of amine groups can also be estimated using a simple model in which roughly spherical proteins cover the top half of the cylindrical nanotube. The proteins are assumed to coat the available nanotube surface with amine groups proportional to the surface area in contact. The nanotube under consideration here has a diameter of 24 nm (as reflected in the small bandgap observed in Fig. 7a), so that the surface area in contact with each 5 nm protein is  $\pi/2 \times 2.4 \times 5 \text{ nm}^2$ . Each protein surface contains 100 amine groups distributed over the 5 nm sphere, so that on average each protein contacts the nanotube with 20 amine groups. Since the proteins are 5 nm in diameter, we assume that 200 proteins are adsorbed on the 1 μm nanotube. Thus the monolayer of adsorbed protein contacts the nanotube with 4000 adsorbed amine groups, again in good agreement with what one finds by examining the transistor charge characteristics

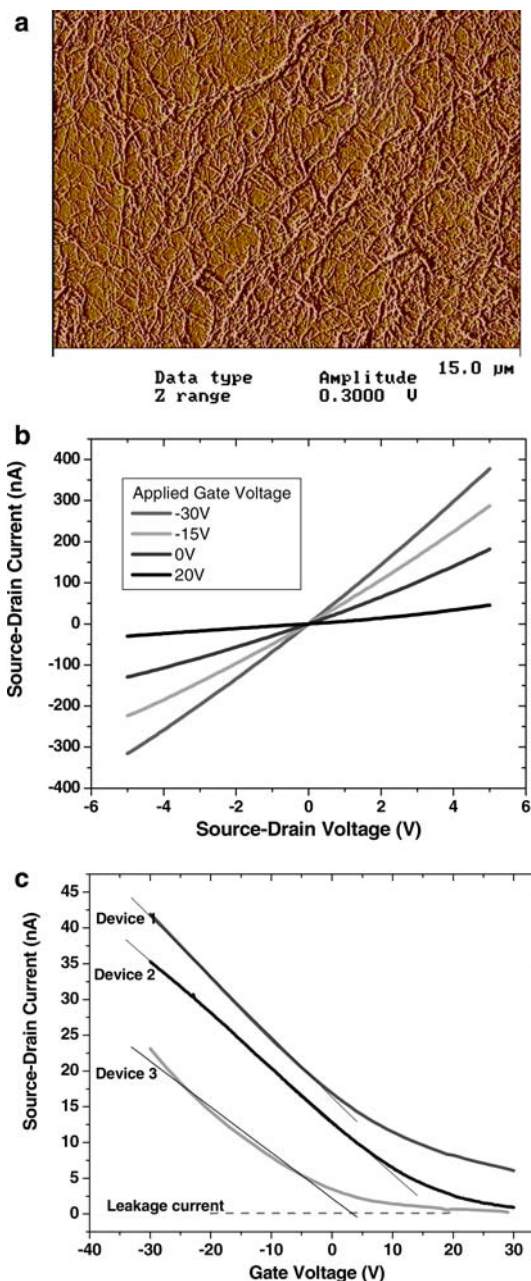


**Fig. 3a–c** Nanotube network transistor. The configuration is the same as that of Fig. 1, with the difference that a nanotube network connects the *S* and *D* electrodes. **a** AFM image of the network, **b** the source–drain current versus the source–drain voltage for different gate voltages, **c** the source–drain current (referred to as the “device characteristics, *DC*”) versus the gate voltage, for transistors with different network densities [32]

metallic contact—the so-called Schottky barrier—may vary substantially from device to device. In an alternative device architecture, the devices contain a random array of nanotubes functioning as the conducting channel, as shown in Fig. 3. Current flows along several conducting channels that determine the overall device resistance. In this configuration, the device operation depends upon the density of nanotubes. For a dense array, screening of the gate voltage by the conducting

nanotubes is important, in a fashion similar to gate voltage screening due to a metal layer deposited on the device. For a rarified array, such screening is not significant and the array can serve as the source-to-drain conducting channel. It is expected that arrays close to and on the conducting side of the two-dimensional percolation limit will have appropriate transistor characteristics. Under such circumstances screening effects are expected to be small, but conduction is still provided by the nanowire network. Devices with nanotube network conducting channels, while less sensitive than single nanotube devices, offer reproducibility and manufacturability. In both device architectures, the parameter that is used for detection is the so-called device characteristic (DC), the dependence of the source-drain current,  $I_{sd}$  (for a fixed source-drain voltage  $V_{sd}$ ), on the gate voltage,  $V_G$ . A typical DC is displayed in Fig. 3. As a rule the device also displays hysteresis, due to mobile ions at the surface of the device. In the following figures, such hysteresis will be shown only if relevant to the observations; otherwise only gate voltage sweeps in one direction—as in Fig. 3c—with be displayed.

---

### Detection schemes

Several different detection schemes can be employed for biosensing applications. The presence of an immobilized biomolecule, or the reaction between biomolecules (such as a ligand-receptor binding for example) can be followed by examining the change in the device characteristics after the biomolecule is immobilized, the reaction is completed and the buffer is removed. The DC is measured in a conventional configuration, applying the bottom gate (called “bottom gating”), as shown in Fig. 2a. This is appropriate if only the mere presence of the biomolecule, or the completion of the biological reaction is examined; such a method may be appropriate for a variety of biotechnology applications. It is much preferable, however, to monitor the biological processes that take place in an appropriate buffer environment. Real-time signal acquisition and analysis may have significant impact on the biological sciences for several reasons. First, the time scales for biological processes may be measured directly. The time taken for a protein to undergo conformational changes or DNA duplex formation and its complement to form a duplex could be measured directly. Second, the electronic data may produce electronic signatures specific to a biological process. For example, if each binding of a different antigen to an antibody results in a particular electronic signature, then the different antigens may be distinguished from each other. This could dramatically alter the landscape of biological sensing, and aid the development of practical biosensors by solving the problems of false positives and poor cross-sensitivities. Biomolecules undergo a variety of fluctuations and conformational changes that span several orders of magnitude.

Picosecond time scales characterize intramolecular vibrations [33], with anharmonic relaxations [34] on the order of nanoseconds. Protein collapse occurs at milliseconds to seconds [35–40]. The internal time constant of our devices is on the order of microseconds, allowing signal processing at time scales exceeding this limit.

The fact that the physiological buffer is conductive offers an alternative detection scheme [41]<sup>3</sup> to the conventional gating configuration shown in Fig. 2. An electrode is applied to the liquid and  $I_{sd}$  is measured as function of the voltage on the electrode, as depicted in Fig. 4a. Several precautions must be taken. Electrochemical reactions may occur at large gate voltages. These can be identified (and avoided) by monitoring the current between the gate and the conducting channel. The source and drain electrodes and all the conducting leads must be isolated from the buffer in order to avoid non-desirable reactions. A typical DC for both “liquid gating” and “bottom gating” is shown in Fig. 4b. The two configurations result in a similar DC if an appropriate scaling of the  $x$ -axis is performed. This scaling is due to the different dielectric layers in the two cases: an oxide insulating layer for bottom gating and a hydration layer in the case of “liquid gating”. Monitoring the change in the DC versus time, as shown in Fig. 4c, allows real-time monitoring of the attachment of the protein to the device.

---

### Interaction of the devices with the environment

The transistor configuration where the conducting channel is a carbon nanotube is different from usual transistor configurations: in the former case the most sensitive element of the device, the conducting channel, is open to the environment. In addition, because of the tubular structure of the nanotube, all the current flows at the surface of the channel, in direct contact with the environment. As a result, these devices are extremely sensitive to environmental factors, such as the presence of different chemical and biological species in the vicinity of the device. The interaction of devices with various inorganic species has been explored in detail, and such experiments serve as useful benchmarks for the effects that are observed when the environment is modified. Both exposure to gases and to coating layers has been studied.

Consider a molecule in the vicinity (usually at the surface) of the nanotubes that form the conducting channel. The effect of such a molecule may be similar to the effect of an impurity in a conventional semiconductor, with two consequences. There may be a charge transfer from the molecule to the nanotube channel, and

---

<sup>3</sup>Detailed experiments performed by us (M. Briman and G. Gruner, to be published) using a setup similar to described in [41, 42] demonstrate that conduction through the buffer leads to negligible effect. The transistor characteristics, however, depend on the pH, and such dependence has to be taken into account when the effect of biomolecules on the transistor characteristics is evaluated.

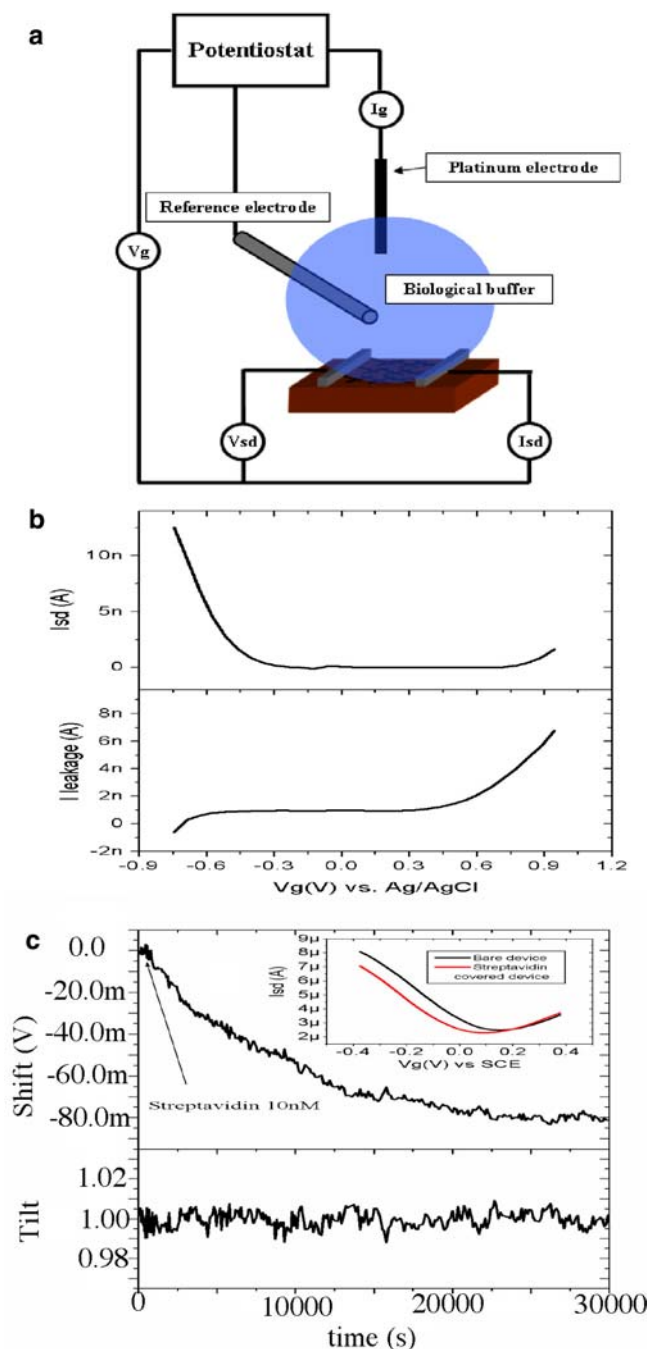


**Fig. 4a–c** **a** Device arrangement for “liquid gating”, as described in the text. Instead of a gate provided by a (*doped*) silicon layer, as shown in Fig. 1, the gating is accomplished by immersing a Pt electrode in the conducting liquid that surrounds the network and the source and drain electrodes. **b** Device characteristics (*upper figure*) and the so-called *leakage current* (measured between the Pt electrode and the S/D electrodes). The finite leakage current indicates the onset of electrochemical reactions. **c** Shift in the DC versus time during incubation with streptavidin. The slope (*tilt*) of the DC is not affected by the presence of streptavidin, indicating charge transfer between the biomolecule and the nanotube channel (see also Fig. 5)

at the same time the molecule may act as a scattering potential. The consequences of the two effects are different: a charge transfer to the nanotube shifts the DC

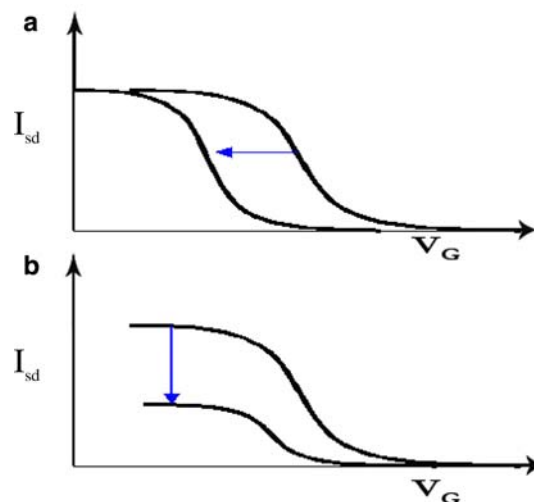


**Fig. 5a–b** Change in the transistor device characteristics (DC) in the presence of an adsorbed species S. **a** The effect of electron transfer from S to the nanotube, **b** potential scattering (reducing the carrier mobility) of charge carriers by the scattering potential created by S

towards more positive (electron donation from the molecule to the nanotube) or negative (hole donation) gate voltages. In contrast, a molecule acting as a scattering center (without a charge transfer) leads to a decrease in the mobility, thus suppressing the current without shifting the characteristics. Such a suppression may also occur through a mechanical distortion of the nanotube. The two situations are shown in Fig. 5. Both may occur, and the transistor configuration allows the separation of the two factors (the change in the carrier density and/or mobility). In Fig. 4c for example, the presence of the biomolecule streptavidin leads to a shift in the device characteristics (similar to that shown in Fig. 5a), indicating a charge transfer from streptavidin to the nanotube.

#### Interactions of devices with gases: examining the response to the environment

Upon exposure to various gases, one finds a shift in the DC, towards either more negative or positive gate voltages, indicating a charge transfer from or to the nanotube from the molecule residing on its surface (note that in the case of gases, the molecules hop on and off the nanotubes, and the time average is recorded). This effect has been studied in detail. Figure 5a shows the effects for electron-donating ( $\text{NH}_3$ ) and electron-withdrawing ( $\text{NO}_2$ ) species [43]; the shift in the device characteristics strongly suggests a charge transfer between the adsorbed molecules and the nanotubes. Although, the notion that the effect is due to the charge transfer is not universally accepted, unpublished calculations strongly suggest that this is the case. The responses of these devices to ammonia have also been studied in water [5], and the shift in the DC is displayed in Fig. 6b

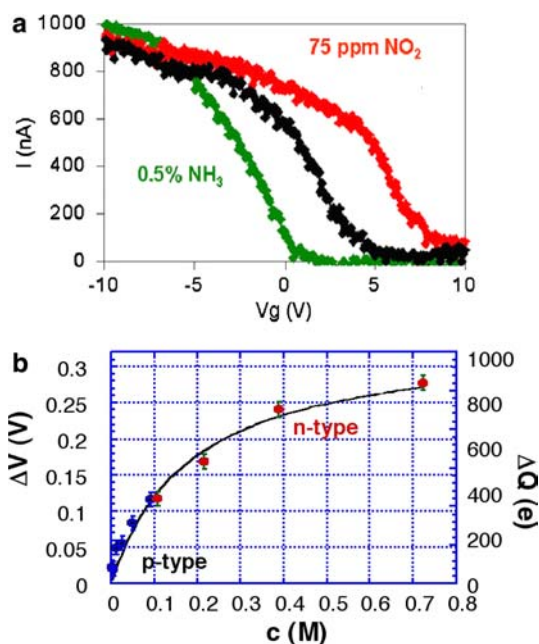


**Fig. 6a–b** a Effects of electron-donating  $\text{NH}_3$  and electron-withdrawing  $\text{NO}_2$  on the transistor device characteristics. The *black symbols* correspond to the DC in air. **b** The shift in the device characteristics,  $\Delta V$ , upon exposure to  $\text{NH}_3$  in water, for different  $\text{NH}_3$  concentrations [27]

for different ammonia concentrations. The full line depicts the expected theoretical curve for weak binding of  $\text{NH}_3$  molecules. Under such circumstances the molecules hop on and off the channel, creating a dynamic equilibrium. The coverage of the devices—assuming that the change (in this case the shift of the DC) is proportional to the coverage, the shift—can be calculated as a function of the  $\text{NH}_3$  concentration in the liquid. The full line in Fig. 6b represents this calculated dependence, which fits the experimental observations quite accurately. These experiments also confirm that the main effect due to  $\text{NH}_3$  is charge transfer from the molecule to the nanotube channel, with scattering effects (see Fig. 5) playing a lesser role. The charge donated can also be estimated [5], leading to the conclusion that each adsorbed  $\text{NH}_3$  molecule donates 0.04 electrons to the nanotube conducting channel.

#### The effect of a polymer coating on the DC

The devices have also been coated with various, mainly polymer, layers in order to change the device characteristics and achieve the desired defined functionality. Both poly(ethylene) glycol (PEG) and poly(ethylene) imine (PEI) have been explored due to their biofunctionality. A PEG layer has little influence on the DC, while PEI dramatically changes the DC. The effect of adsorbed amines on the electronic properties of nanotubes has been studied by several authors [43, 44]. The most quantitative measurement has shown that a proportion of the electrons per adsorbed amine, roughly

comparable to the electrons donated by the  $\text{NH}_3$  groups, are donated to the semiconducting nanotubes. This charge donation is detected as a shift in the threshold voltage of the nanotube transistor towards negative gate voltages. In addition, geometric considerations lead to the conclusion that a  $1 \mu\text{m}$  nanotube adsorbs 20,000–75,000 amine groups from PEI. These numbers can be used as calibration points when the charge transfer between biomolecules and devices is estimated.

#### Interactions between devices and biomolecules

Interactions between electronic devices and biological matter are fundamental to biosensing [45] and bioelectronics [46]. A major goal continues to be the fabrication of structures with proteins immobilized on various functional surfaces, while preserving the biological activity of the proteins [47, 48]. A variety of mechanisms have been explored for immobilization, including covalent bonding [49], hydrophobic interactions, and charge transfer-induced adsorption [50]. The most direct evidence has been provided by scanning force microscopy, which in recent years has been used to measure the strength of protein attachment to a variety of surfaces [51]. Interactions between biomolecules and various surfaces have been widely utilized, but these interactions between surfaces and biomolecules are not well understood. Interrogation of the device characteristics before

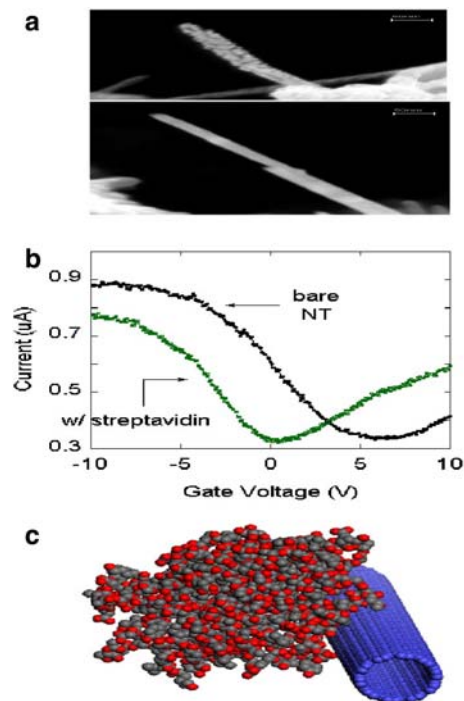


**Fig. 7a–c** a Multiwall carbon nanotube before and after incubation with biotinylated bovine serum albumin (BBSA). **b** Effect of nonspecific streptavidin binding on the device characteristics. The shift in the DC indicates charge transfer from streptavidin to the nanotubes. **c** The NT-streptavidin complex (29)

and after immobilization offers an opportunity to identify some of these interactions.

### Proteins immobilized on a device

We have used biotinylated bovin serum albumin (BBSA) and similar proteins to examine the immobilization, and electronic detection of the immobilized species. SEM images give clear evidence (Fig. 7a) of nonspecific protein binding to nanotubes. Such protein immobilization on nanotubes has been observed before by other groups and is by itself not surprising, given the good size compatibility of the two entities. We made similar observations for streptavidin and a range of other proteins. These images also confirm a strong binding between the nanotubes and proteins. Unlike ammonia discussed earlier, once a protein is bound to the nanotubes, it will remain bound to the device under ambient conditions. Various contributions to the bindings have been suggested, with hydrophobic interactions as the main source of immobilization. Streptavidin is a tetrameric protein of  $M_r$  64,000 [52]. According to electrophoretic measurements, it is electrically neutral at pH values between 6 and 7.2. However, it contains a number of residues with strong side chain bases [52–56]. Each streptavidin monomer has two histidine residues. His-87 is located close to the biotin-binding pocket on the “top” and “bottom” of the protein, and His-127 residues lie on the long side of the barrel at the interface between two subunits. Histidine is one of the strongest bases at physiological pH (7.0), and it plays a major role in streptavidin’s recognition of biotin [52]. For other important base-containing residues, such as lysine and arginine, only some of the residues have been specifically located in the tertiary structure. Based on those locations that have been identified, one can estimate that the external envelope of the protein contains 80 arginine residues and 20 lysine residues, giving a total of 100 electron donating amine groups. This suggests that—as with PEI—electron donation from the biomolecule to the device may play a significant role in the binding.

Streptavidin binds to the nanotubes strongly [20], with full coating of the devices after incubation for a few hours. The observation of a shift in the DC when the devices are “coated” with streptavidin (Fig. 7b) indicates that charge transfer plays a role in protein adsorption. Given the capacitance [41] between the nanotube and the gate, the quantity of charge donated by the proteins can be related to the observed threshold shift. Using the size of the streptavidin and the geometry of the device, the total number of amine groups can be estimated. Assuming that each group donates 0.04 electrons, this represents a quantity  $Q=17$  AC of donated charge. Using straightforward electrostatics, one can estimate the shift in the transistor characteristics, obtaining  $-50$  V. By comparison, the observed threshold shift in the presence of a

monolayer of protein in buffer is  $-60 \pm 3$  mV, in good agreement with the estimated value given above. Alternatively, the amount of charge transferred can be estimated using the calibration provided by measurements of ammonia and PEI adsorption, and one finds values similar to that given above [19]. Experiments on streptavidin as well as other proteins indicate that charge transfer interactions between proteins and carbon nanotubes play an important role in immobilization.

### The effect of viruses on device characteristics

One expects that, because of their surface proteins, viruses also readily interact with devices and are immobilized. This has been partially confirmed by experiments using the plant virus CCMV. As with protein adsorption, one observes a shift (Fig. 8) in the DC, indicating charge transfer from the surface proteins to the device. The effect, however, is surprisingly small; about an order of magnitude smaller than in the case of streptavidin. It appears that binding of the surface proteins to the device is weak, and binding is also hampered by the geometric arrangement of the surface proteins due to their position within the virus structure. Moreover, this difference is highly virus-specific. Binding of the virus T4 leads to a significantly smaller effect than for CCMV. This is not surprising considering the

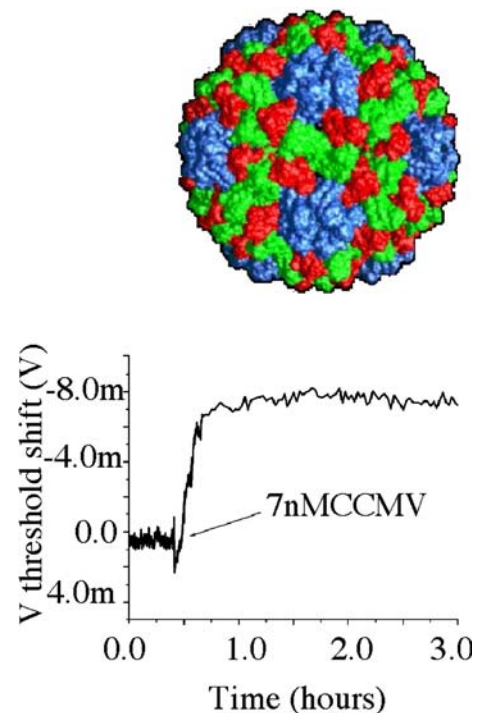


**Fig. 8** Shift in the device characteristics versus time for a device incubated with the plant virus CCMV (also shown). The response is highly virus-specific and also depends upon the buffer characteristics

significant structural and chemical differences between the two viruses.

### Sensing biological processes using nanotube FET devices

The examples described above illustrate the interaction between the biomolecules and the electronic devices. The experiments summarized previously also provide important insights into biomolecule immobilization issues, and lay the groundwork for the electronic detection of biological processes. Two examples given below—the detection of ligand-receptor binding and the detection of an enzymatic reaction—take the concept of the electronic detection of biological reactions one step further.

#### Ligand–receptor interactions

Monitoring specific interactions between biomolecules remains one of the most important objectives of biosensing [57–59]. A detection scheme that involves electronic detection is shown in Fig. 9a. First, a polymer layer is applied to the device in order to avoid nonspecific biomolecule binding. A ligand is then attached to the layer. Such a ligand serves as the recognition site through ligand-receptor binding. Finally, the resulting structure is incubated with the receptor in order to explore the binding process. All of these steps can be followed readily by examining the device characteristics after each step. The scheme is expected to work for a broad variety of interactions, and may be appropriate even for detecting DNA duplex formation. A PEI/PEG

layer was used, along with biotin as the ligand and gold-labeled streptavidin as the receptor [57]. We have found that the PEI/PEG layer effectively prevents (in contrast to what we have found in non-functionalized nanotubes) the binding of streptavidin to the device. After polymer coating, biotin was covalently attached to the polymer and the device was subsequently incubated with gold nanoparticle-labeled streptavidin. The SEM image shown in Fig. 9b is the realization of the architecture, and of the end-result of the incubation process. The image clearly shows the gold particles along the nanotube, giving evidence of streptavidin binding onto the nanotube in question. With an 800 nm-long nanotube, and a gold sphere diameter of 10 nm, it is expected that there are approximately 80 streptavidin molecules in direct interaction with the nanotube-conducting channel after full coating. This estimate is in good agreement with what one concludes through direct examination of the image. Biotin-streptavidin binding has been detected by changes in the device characteristics. The resulting change in the DC is displayed in Fig. 10a. Instead of a shift in the DC, one observes a suppression of the conduction, most likely due to some distortion of the nanotube caused by the presence of streptavidin. Model

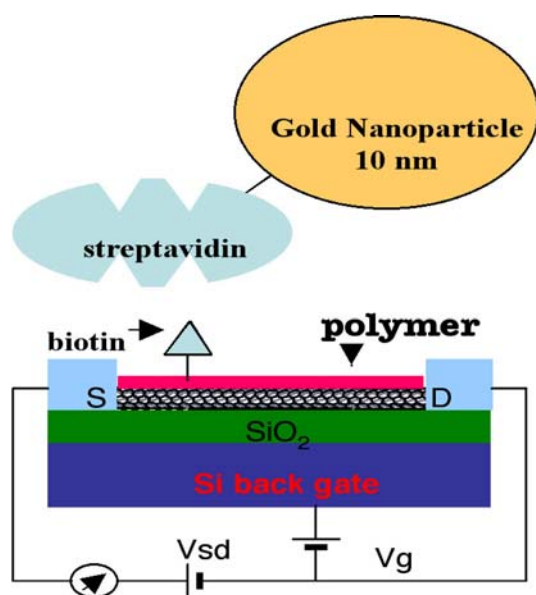


**Fig. 9** Detection scheme for biotin–streptavidin ligand receptor binding. The device is coated with a PEG/PEI polymer that prevents non-specific binding of streptavidin. A biotin is attached via a tether to the polymer

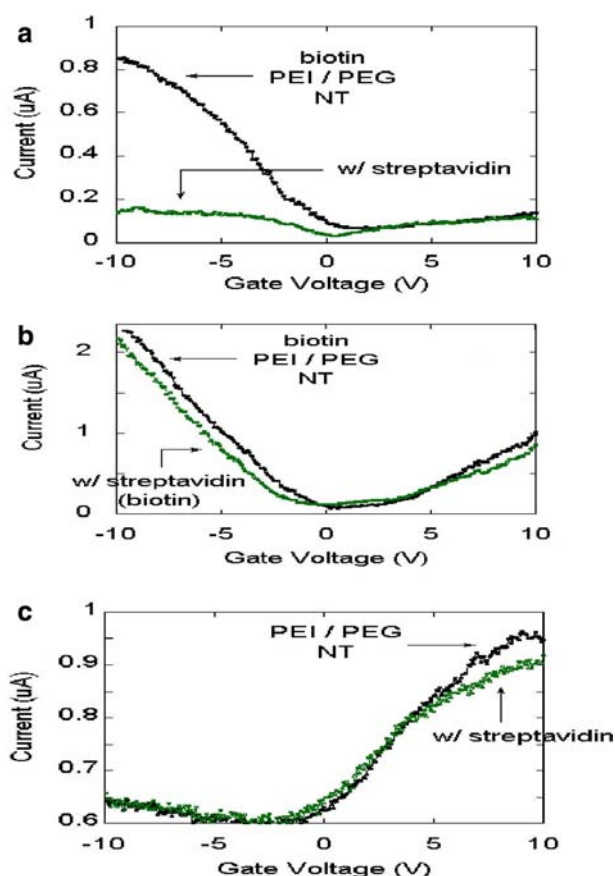


**Fig. 10a–c** Ligand receptor binding between biotin and streptavidin. **a** Response of device shown in Fig. 9. **b** Control experiment involving biotinylated streptavidin. **c** Control experiment using the device shown in Fig. 9, but without biotin attachment (57)

calculations indicate that even extremely small distortion leads, by disruption of the periodicity of the atomic structure of the nanotube, to carrier scattering, and to a reduction in carrier mobility in the conducting channel. The change exceeds the noise limit by a factor of approximately 10, leading to the conclusion that the current detection limit is about ten proteins. Various control experiments have also been conducted. Non-specific binding was electronically detected for streptavidin (Fig. 7), but—as discussed above—a PEI/PEG layer was found to prevent nonspecific binding, and indeed no change in the device characteristics was found when polymer-coated devices were incubated with streptavidin and other proteins (Fig. 10c). Control experiments involving biotinylated streptavidin, with the binding sites already occupied by biotin, did not (as expected) result in binding. This is highlighted by the fact that the device characteristics did not change upon incubation with biotinylated streptavidin (Fig. 10b).

### Enzymatic reactions

One example of the application of devices to the electronic monitoring of an enzymatic reaction [60–62] is the enzymatic hydrolysis of starch [63, 64–66]. Starch consists of a linear component, amylose, which is composed of linkages between D-glucopyranose residues and amylopectin. We have characterized starch enzymatic hydrolysis with amyloglucosidase [67] in acidic buffer, resulting in complete cleavage of the polymer to water-soluble glucose. The starch-covered single wall nanotubes (SWNT) were also studied by

transmission electron microscopy. Figure 11a shows a high-resolution electron transmission (HRTEM) image of SWNT covered with starch. For imaging purposes, the starch was contrasted using a  $\text{RuO}_4$  staining procedure. After starch deposition, the DC shifts by approximately  $\sim 2$  V towards negative gate voltages (Fig. 11b), corresponding to electron doping of the nanotube channel by the polymer. Compared to other polymers, such as poly(ethylene imine) (PEI), the magnitude of the shift is small. This fact, most likely, relates to the difference between the electron donating abilities of the alcohol and ether groups in starch as compared to the electron donating abilities of the amines in PEI. After the enzymatic reaction was completed on the starch-functionalized device, the device response observed before starch deposition (Fig. 4b) was recovered, indicating that during the enzymatic reaction all of the starch is hydrolyzed to glucose, with the hydrolysis product washed off prior to the electronic measurements. Two control experiments were performed to confirm these results. First, the starch-functionalized chip was rinsed with buffer to see if the buffer alone could wash away the starch deposited on the device. The DC after rinsing with buffer solution was similar to that obtained before rinsing, leading to the conclusion that starch removal does not occur using buffer alone. Another control experiment involved the deposition of enzyme solution on bare devices. The DC showed increased hysteresis, but no significant shift was observed, indicating that the presence of enzymes alone do not lead to charge transfer.

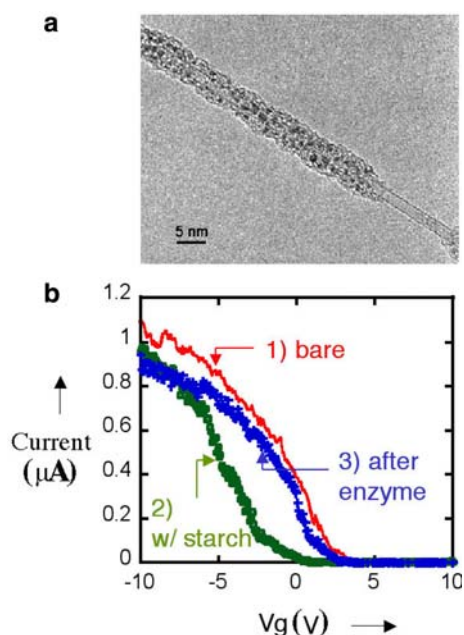


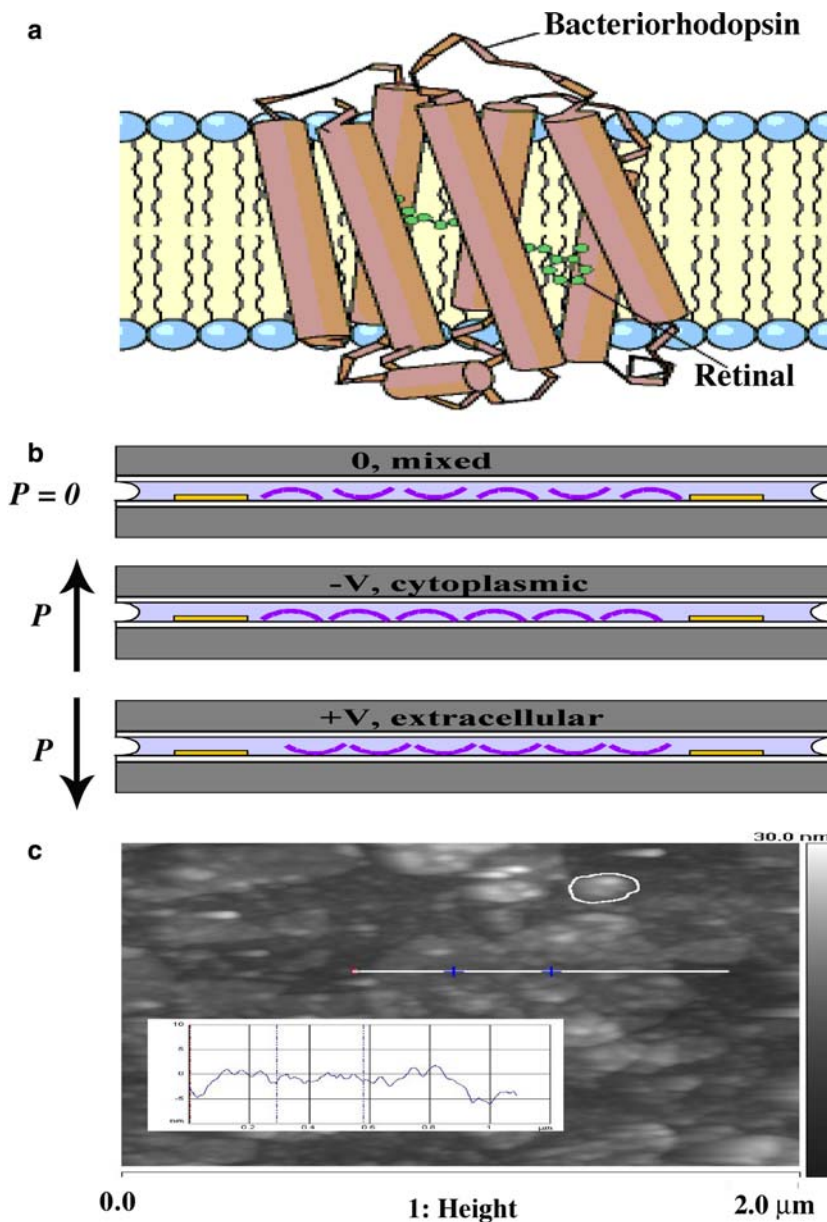
**Fig. 11a–b** Enzymatic degradation of starch. **a** Starch-coated nanotube; **b** device characteristics before and after starch deposition and after the enzymatic degradation of starch [63]

### Bioelectronic integration: bacteriorhodopsin (bR) in a purple layer

The next example involves a bioentity with a well-defined biological function—a protein-membrane complex [68]. We chose to use the purple membrane (PM) from *Halobacterium salinarum* [69], which has been widely studied. PM contains the light-sensitive membrane protein bacteriorhodopsin, which serves as a photochemical proton pump and has been used to fabricate photo-transistors. The structure is depicted in Fig. 12a. In addition, rhodopsin has a permanent electric dipole moment, a charge distribution, which produces an electric field pointing from the extracellular side of the membrane towards the cytoplasmic side [68]. These properties make PM an ideal prototype membrane for nanobioelectronic integration. In particular, we use the dipole as an indicator that the integration preserves the biomaterial while bringing it into contact with the nanoelectronic device.

PM isolated from *H. salinarum* [69, 70] was deposited on devices. To observe the effect of the electric dipoles fixed in the PM, devices were prepared in three conditions, as shown in Fig. 12b: with the cytoplasmic side of the PM facing the nanotubes [71], with the extracellular

**Fig. 12a–c** **a** Illustration of bacteriorhodopsin in a purple membrane. **b** Three purple membrane (PM) arrangements—random, cytoplasmic and extracellular—deposited by employing voltages of 0,  $-3$  and  $+3$  V, respectively. The gray areas correspond to two Si chips, and the voltages were applied between the two chips. The voltages listed correspond to the potential on the top chip. **c** AFM image of deposited PM; the scan indicates the height of the membrane,  $\sim 5$  nm [68]



side facing the nanotubes, and with a mixture of both orientations [72, 73]. The particular orientation required was achieved by applying a particular gate voltage (as described in Fig. 12) of  $+3$  or  $-3$  V. The voltage leads to an electric field orientation that depends upon the voltage polarity at the nanotube network surface. Changes due to interactions with the electric dipoles of the bR in the purple membrane are most likely responsible for the gate voltage-influenced deposition.

The structure we have examined is a dense network of individual carbon nanotubes (Fig. 3a) covered by the membrane, referred to earlier as a nanotube network field-effect transistor. The deposition of purple membrane has been examined by AFM imaging, and one image is shown in Fig. 12c. One observes layers 5 nm in height, corresponding to a single layer of the membrane.

This configuration has several significant features. First, the cell membrane is in direct contact with the semi-conducting channel of the transistor. This is distinct from previous work, in which cell membranes have contacted the gate electrodes of transistors [31]. In this configuration, transistors detect the electrical potential across membranes; in contrast, our devices detect local electrostatic charges on the biomolecules. Second, the use of a large number of nanotubes ensures that entire patches of membrane are in contact with nanotubes.

Figure 13 highlights the device parameters before and after deposition for a typical device upon the application of  $+3$  V (resulting in the cytoplasmic side of the membrane facing the device surface). An opposite but significantly smaller effect is observed with the extracellular side interfacing with the device. The changes

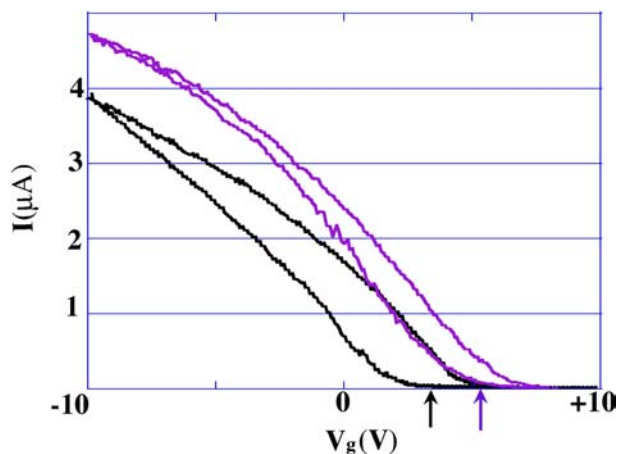


**Fig. 13** Device characteristics for a device before (*black*) and after (*purple*) the deposition of cell membrane at +3 V. A clear shift in the device characteristics to positive gate voltages is observed. A shift in the opposite direction (but of a smaller magnitude) is observed for membrane deposition at negative voltages

were observed repeatedly in several devices prepared in the same way, and show that the PM was successfully integrated with the devices.

The changes in the response of the device (including the change in the hysteresis upon deposition of the PM) can be analyzed in terms of our understanding of the operation of these devices [74, 75]. The shift in device characteristics results from the electrostatic field associated with the bacteriorhodopsin electric dipole. This field induces charge in the nanotubes [76], leading to the changed device characteristics discussed before (see also [77–79]). Consequently, one can examine and analyze the change in the device response, and the significant difference caused by the cytoplasmic and extracellular orientations. In addition to the opposite change in the DC observed for the two orientations, the magnitude of the change is also different, providing evidence of a different charge and/or dipole arrangement in the two cases. Such an asymmetry is known to exist<sup>4</sup>, in that the dipole is closer to one side of the PM than the other [80]. Here we are able to observe this asymmetry directly because of the device configuration, in which the PM contacts the nanotubes directly. One can quantify the asymmetry by modeling the electrostatic effect of the bacteriorhodopsin dipole on the nanotubes<sup>5</sup>, and this model is depicted in Fig. 14. The dipole is still not well understood, but is known to result from the competition between several charge distributions, resulting in a net dipole moment of  $3.3 \times 10^{-28}$  C m per rhodopsin monomer. To calculate the effect of this dipole on the

<sup>4</sup>This asymmetry is reflected in the large amount of charge induced in mixed-orientation devices, since without an asymmetry, the charge induced by equal amounts of cytoplasmic-oriented and extracellular-oriented PM should cancel.

<sup>5</sup>The background charge due to the phosphate heads of the lipids is 0.2 electrons per square nanometer [25], which is too weak to explain the charge induced in our devices.

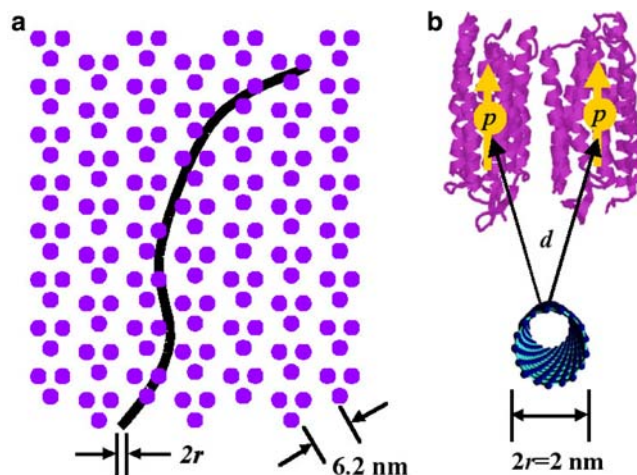


**Fig. 14a–b** **a** Model shows the geometry of the PM (purple membrane) with respect to the nanotubes. Rhodopsin (*purple dots*) assembles into trimers, which are arranged on a hexagonal lattice. The nanotube is a *curved line*. **b** Model shows the dimensions used in the calculations. A rhodopsin monomer situated near a nanotube has a dipole moment  $p$ . This point dipole is situated within the rhodopsin at a distance  $d$  from the nanotube surface

nanotubes, we can use a simple electrostatic model in which the rhodopsin molecules above a nanotube (Fig. 14) form a line of constant dipole density. Such a model, when combined with the observed changes in the device characteristics, allows one to evaluate the location of the dipole moment of bR within the purple layer.

Several important conclusions can be reached from these experiments. First, the functionality of the electronic device is preserved. Second, the PM remains intact as a layer, and the bacteriorhodopsin membrane proteins retain their electric dipoles. Third, the deposited PM has been demonstrated to contact the device directly and to interact with its electrical properties. In addition, analysis of the electrical properties of the device allows us to gain information on some characteristics of the biomolecule—in this case the location of the dipole within the molecule.

The experiments represent the first attempt to integrate biosurfaces with active electronic devices. We find that after integration the components retain their functionality—a significant finding, with implications for the field of bioinorganic interfaces. In addition, our results provide additional details about the asymmetry of the bacteriorhodopsin charge distribution.

## Conclusions

The nanoscale electronic devices—field effect transistors with carbon nanotube conducting channels—that we have fabricated readily interact with the environment. For a variety of species, such as reactive gases, polymers with reactive chemical groups and also various proteins and viruses that have been studied, our experiments

demonstrate that charge transfer occurs between the species and the device. The change in the device characteristics, DC, allows the estimation of the transferred charge for each species. Our observations on proteins also suggest a strong charge transfer from the protein to the nanotube channel. The charge transfer interaction mechanism we have identified for proteins may have implications for a broad range of fields where immobilization is attempted and used for fundamental studies and also for applications. Such interactions also involve functional groups that are different than those involved in hydrophobic interactions, and thus may lead to different attachment geometries in the two cases. Experiments involving a variety of proteins may shed light on some of the issues raised in here.

It is also apparent that we know enough about nanoelectronics to be able to use a nanodevice as an investigative tool. We can use these devices to monitor a variety of biologically-significant reactions. This is possible because most of these reactions involve local electric fields and charge rearrangement. The examples given above also clearly indicate the potential applicability of the devices to various biotechnological fields. The next step in this direction is to examine device operation in a serum and to explore the sensitivity and specificity issues that arise in application areas such as early detection of cancer. As discussed before, the devices have extreme sensitivities, with single molecule detection clearly in sight. Such sensitivity may also lead to detection schemes that do not require amplification before detection, with nanotube-based transistors having a clear advantage: while other conventional transistors or devices with nanowire components are also inherently sensitive, they do not match the sensitivity of carbon nanotube FETs<sup>6</sup>. It is evident that the results discussed here only represent the first step towards a viable approach to biosensing. Further work is needed to evaluate the operation of the device in a serum environment, to confirm detection with the required specificity in the presence of a multitude of biomolecules, and to establish the necessary (analyte-dependent) sensitivity of the method.

We have also used the interaction between a biological system and a nanodevice to learn not about the electronic component but about the biological component. As a result, it should be possible to connect living cells directly to these nanoelectronic devices, and the above concepts could conceivably be extended at a later stage to include what one could call “cellectronics”—cell-based electronic sensing—measuring the electronic responses of living systems, as well as to using nanoscale devices for in vivo applications: studying cell physiology, medical screening and diagnosis. The architectures of the sensors can be turned into devices

where—by applying a voltage between elements of the sensor—surface charges can be created on the sensing element where the biomolecules are immobilized. Such surface charges will interact with the charged biomolecules, but these potentially important effects have not been explored to date. The small size of the nanotube device also allows integration of such devices into living organisms. This could allow in vivo electronic detection of biological processes.

**Acknowledgements** Many of the experiments reported here were performed by K. Bradley, M. Briman, A. Star, and the devices were fabricated by J.C. Gabriel and D. Hecht. This work was partially supported by the National Science Foundation Grant no. 0415130. Many of the experiments were performed at Nanomix Inc., the company where the author was Chief Scientist.

## References

1. Robers M, Rensink IJAM, Hack CE, Aarden CE, Reuteling-sperger CPM, Glatz JFC, Hermens WT (1999) A new principle for rapid immunoassay of proteins based on in situ precipitate-enhanced ellipsometry. *Biophys J* 76:2769
2. McNeil CJ, Athey D, Wah OH (1995) Direct electron transfer bioelectronic interfaces application to clinical analysis. *Biosens Bioelectron* 10:75
3. Willner I (2002) Bioelectronics biomaterials for sensors, fuel cells, and circuitry. *Science* 298:2407
4. Hu H, Ni Y, Montana V, Haddon RC, Parpura V (2004) Chemically functionalized carbon nanotubes as substrates for neuronal growth. *Nano Lett* 4:507
5. Pantarotto D, Partidos CD, Graff R, Hoebeke J, Briand J-P, Prato M, Bianco A (2003) Synthesis structural characterization and immunological properties of carbon nanotubes functionalized with peptides. *J Am Chem Soc* 125:6160
6. Zheng M, Jagota A, Strano MS, Santos AP, Barone P, Chou SG, Diner BA, Dresselhaus MS, Mclean RS, Onoa GB, Samsonidze GG, Semke ED, Usrey M, Walls DJ (2003) Structure-based carbon nanotube sorting by sequence-dependent DNA assembly. *Science* 302:1545
7. Richard C, Balavoine F, Schultz P, Ebbesen TW, Mioskowski C (2003) Supramolecular self-assembly of lipid derivatives on carbon nanotubes. *Science* 300:775
8. Fritz J, Cooper EB, Gaudet S, Sorger PK, Manalis SR (2002) Electronic detection of DNA by its intrinsic molecular charge. *Proc Natl Acad Sci USA* 99:14142
9. Zayats M, Raitman OA, Chegel VI, Kharitonov AB, Willner I (2002) Probing antigen-antibody binding processes by impedance measurements on ion-sensitive field-effect transistor devices and complementary surface plasmon resonance analyses: development of cholera toxin sensors. *Anal Chem* 74:4763
10. Kharitonov AB, Zayats M, Lichtenstein A, Katz E, Willner I (2000) Enzyme monolayer-functionalized field-effect transistors for biosensor applications. *Sens Actuat B Chem* 70:222
11. Pouthas F, Gentil C, Côte D, Bockelmann U (2004) DNA detection on transistor arrays following mutation-specific enzymatic amplification. *Appl Phys Lett* 84:1594
12. Li Z, Chen Y, Li X, Kamins TI, Nauka K, Williams RS (2004) Sequence-specific label-free DNA sensors based on silicon nanowires. *Nano Lett* 4:245
13. Wang WU, Chen C, Lin K-H, Fang Y, Lieber CM (2005) Label-free detection of small-molecule-protein interactions by using nanowire nanosensors. *Proc Natl Acad Sci USA* 102:3213
14. Hahm JI, Lieber CM (2003) Direct ultrasensitive electrical detection of DNA and DNA sequence variations using nanowire nanosensors. *Nano Lett* 4:51

<sup>6</sup>For example, biotin-streptavidin binding has been measured using nanowire-based [81] and carbon nanotube-based [82] devices. While a few percent change is observed using nanowires, the binding leads to an order of magnitude change when carbon nanotube-based transistors are used.

15. Saito R, Dresselhaus G, Dresselhaus MS (1998) Physical properties of carbon nanotubes. Imperial College Press, London
16. Shim M, Shi Kam NW, Chen RJ, Li Y, Dai H (2002) Functionalization of carbon nanotubes for biocompatibility and biomolecular recognition. *Nano Lett* 2:285
17. Huang W, Taylor S, Fu K, Lin Y, Zhang D, Hanks TW, Rao AM, Sun Y-P (2002) Attaching proteins to carbon nanotubes via diimide-activated amidation. *Nano Lett* 2:311
18. Chen RJ, Zhang Y, Wang D, Dai H (2001) Noncovalent sidewall functionalization of single-walled carbon nanotubes for protein immobilization. *J Am Chem Soc* 123:3838
19. Davis JJ, Green MLH, Allen H, Hill O, Leung YC, Sadler PJ, Sloan J, Xavier AV, Tsang SC (1998) The immobilisation of proteins in carbon nanotubes. *Inorg Chim Acta* 272:261
20. Balavoine F, Schultz P, Richard C, Mallouh V, Ebbesen TW, Mioskowski C (1999) Helical crystallization of proteins on carbon nanotubes: a first step towards the development of new biosensors. *Angew Chem Int Edit* 38:1912
21. Dieckmann GR, Dalton AB, Johnson PA, Razal J, Chen J, Giordano GM, Munoz E, Musselman IH, Baughman RH, Draper RK (2003) Controlled assembly of carbon nanotubes by designed amphiphilic peptide helices. *J Am Chem Soc* 125:1770
22. Martel R, Schmidt T, Shea HR, Hertel T, Avouris Ph (1998) Single- and multi-wall carbon nanotube field-effect transistors. *Appl Phys Lett* 73:2447
23. Bachtold A, Hadley P, Nakanishi T, Dekker C (2001) Logic circuits with carbon nanotube transistors. *Science* 294:1317
24. Collins PG, Bradley K, Ishigami M, Zettl A (2000) Extreme oxygen sensitivity of electronic properties of carbon nanotubes. *Science* 287:1801
25. Kong J, Franklin NR, Zhou C, Chapline MG, Peng S, Cho K, Dai H (2000) Nanotube molecular wires as chemical sensors. *Science* 287:622
26. Star A, Tzong-Ruhan, Gabriel J-CP, Bradley K, Grüner G (2003) Interaction of aromatic compounds with carbon nanotubes. *Nano Lett* 3:1421
27. Bradley K, Gabriel J-CP, Briman M, Star A, Grüner G (2003) Charge transfer from aqueous ammonia absorbed on nanotube transistors. *Phys Rev Lett* 91:218301
28. Cui Y, Wei Q, Park H, Lieber CM (2001) Nanowire nanosensors for highly sensitive and selective detection of biological and chemical species. *Science* 293:1289
29. Bradley K, Briman M, Star A, Grüner G (2004) Charge transfer from adsorbed proteins. *Nano Lett* 4:253
30. Star A, Bradley K, Gabriel J-CP, Grüner G (2003) Nanoelectronic sensors: chemical detection using carbon nanotubes. *Pol Mater: Sci Eng* 89:204
31. Bradley K, Gabriel J-CP, Star A, Grüner DG (2003) Short channel effects in contact-passivated nanotube chemical sensors. *Appl Phys Lett* 83:3821
32. Artukovic E, Kaempgen M, Hecht DS, Roth S, Grüner G (2005) Transparent and flexible carbon nanotube transistors. *Nano Lett* 5:757
33. Larsen DS, Ohta K, Xu Q, Cyrier M, Fleming GR (2001) Influence of intramolecular vibrations in third-order, time domain resonant spectroscopies: 1. Experiments. *J Chem Phys* 114:8008
34. Xie A, van der Meer AFG, Austin RH (2002) Excited-state lifetimes of far-infrared collective modes in proteins. *Phys Rev Lett* 88:018102
35. Arai M, Ikura T, Semisotnov GV, Kihara H, Amemiya Y, Kuwajima K (1998) Kinetic refolding of beta-lactoglobulin studies by synchrotron X-ray scattering, and circular dichroism, absorption and fluorescence spectroscopy. *J Mol Biol* 275:149
36. Pollack L, Tate MW, Finnefrock AC, Kalidas C, Trotter S, Darnton NC, Lurio L, Austin RH, Batt CA, Gruner SM, Mochrie SGJ (2001) Time resolved collapse of a folding protein observed with small angle X-ray scattering. *Phys Rev Lett* 86:4962
37. Kuwata K, Shastry R, Cheng H, Hoshino M, Batt CA, Goto Y, Roder H (2001) Structural and kinetic characterization of early folding events in beta-lactoglobulin. *Nature Struct Biol* 8:151
38. Jones CM, Henry ER, Hu Y, Chan C, Luck SD, Bhuyan A, Roder H, Hofrichter J, Eaton WA (1993) Fast events in protein folding initiated by nanosecond laser photolysis. *Proc Natl Acad Sci USA* 90:11860
39. Lim M, Jackson TA, Anfinsen PA (1997) Modulating carbon monoxide binding affinity and kinetics in myoglobin: the roles of the distal histidine and the heme pocket docking site. *J Biol Inorg Chem* 2:531
40. Lipman EA, Schuler B, Bakajin O, Eaton WA (2003) Single molecule measurement of protein folding. *Kinetics* 310:1233
41. Rosenblatt S, Yaish Y, Park J, Gore J, Sazonova V, McEuen PL (2002) High performance electrolyte gated carbon nanotube transistors. *Nano Lett* 2:869
42. Krüger M, Buitelaar MR, Nussbaumer T, Schönenberger C, Forró L (2001) Electrochemical carbon nanotube field-effect transistor. *Appl Phys Lett* 78:1291
43. Chang H, Lee JD, Lee SM, Lee YH (2001) Adsorption of NH<sub>3</sub> and NO<sub>2</sub> molecules on carbon nanotubes. *Appl Phys Lett* 79:3863
44. Kong J, Dai H (2001) Full and modulated chemical gating of individual carbon nanotubes by organic amine compounds. *J Phys Chem B* 105:2890
45. Robers M, Rensink IJAM, Hack CE, Aarden LA, CPM Reutelingsperger, JFC Glatz, Hermens WT (1999) A new principle for rapid immunoassay of proteins based on in situ precipitate-enhanced ellipsometry. *Biophys J* 76:2769
46. McNeil CJ, Athey D, Ho WO (1995) Direct electron transfer bioelectronic interfaces: application to clinical analysis. *Biosens Bioelectron* 10:75
47. Turner DC, Chang CY, Fang K, Brandow SL, Murphy DB (1995) Selective adhesion of functional microtubules to patterned silane surfaces. *Biophys J* 69:2782
48. Wadu-Mesthrige K, Amro NA, Garno JC, Xu S, Liu G-Y (2001) Fabrication of nanometer-sized protein patterns using atomic force microscopy and selective immobilization. *Biophys J* 80:1891
49. Nicolau DV, Taguchi T, Taniguchi H, Yoshikawa S (1998) Micron-sized protein patterning on diazonaphthoquinone/novolac thin polymeric films. *Langmuir* 14:1927
50. Pompa PP, Blasi L, Longo L, Cingolani R, Ciccarella G, Vasapollo G, Rinaldi R, Rizzello A, Storelli C, Maffia M (2003) *Phys Rev E* 67:41902
51. Sagvolden G (1999) Protein adhesion force dynamics and single adhesion events. *Biophys J* 77:526-532
52. Weber PC, Wendoloski JJ, Pantoliano MW, Salemme FR (1992) Crystallographic and thermodynamic comparison of natural and synthetic ligands bound to streptavidin. *J Am Chem Soc* 114:3197
53. Athappilly FK, Hendrickson WA (1997) Crystallographic analysis of the pH-dependent binding of iminobiotin by streptavidin. *Protein Sci* 6:1338
54. Yaticilla MT, Robertson CR, Gast AP (1998) Influence of pH on two-dimensional streptavidin crystals. *Langmuir* 14:497
55. Wang S-W, Robertson CR, Gast AP (2000) Role of N- and C-terminal amino acids in two-dimensional streptavidin crystal form. *Langmuir* 16:5199
56. Frey W, Schief WR Jr, Pack DW, Chen C-T, Chilkoti A, Stayton P, Vogel V, Arnold FA (1996) Two-dimensional protein crystallization via metal-ion coordination by naturally occurring surface histidines. *Proc Natl Acad Sci USA* 93:4937
57. Star A, Gabriel J-CP, Bradley K, Grüner G (2003) Electronic detection of specific protein binding using nanotube FET devices. *Nano Lett* 3:459
58. Chen RJ, Bangsaruntip S, Drouvalakis KA, Wong Shi Kam N, Shim M, Li Y, Kim W, Utz PJ, Dai H (2003) Noncovalent functionalization of carbon nanotubes for highly specific electronic biosensors. *Proc Natl Acad Sci USA* 100:4984

59. Besteman K, Lee J-O, Wiertz FGM, Heering HA, Dekker C (2003) Enzyme-coated carbon nanotubes as single-molecule biosensors. *Nano Lett* 3:727
60. Schnabel W (1981) Polymer degradation. Henser International, Berlin, Ch 6
61. Wool RP, Raghavan D, Wagner GC, Billieux SJ (2000) Biodegradation dynamics of polymer-starch composites. *Appl Polym Sci* 77:1643
62. Moreno-Chulim MV, Barahona-Perez F, Canche-Escamilla G (2003) Biodegradation of starch and acrylic-grafted starch by *Aspergillus niger*. *Appl Polym Sci* 89:2764
63. Star A, Joshi V, Han T-R, Altoe MVP, Gruner G, Stoddart JF (2004) Electronic detection of the enzymatic degradation of starch. *Org Lett* 6:2089
64. Collins P, Ferrier R (1995) Polysaccharides: their chemistry. Wiley, Chichester, pp 478–523
65. Lehmann J (1998) Carbohydrates: structure and biology. Georg Thieme, Stuttgart, pp 98–103
66. Thompson DB (2000) On the non-random nature of amylopectin branching. *Carbohydr Polym* 43:223
67. Yamamoto T (1994) Enzyme chemistry and molecular biology of amylases and related enzymes. CRC, Boca Raton, FL, pp 3–201
68. Bradley K, Davis A, Gabriel J-CP, Gruner G (2005) Integration of cell membranes and nanotube transistors. *Nano Lett* 5:841
69. Oesterhelt D, Stoerkenius W (1973) Functions of a new photoreceptor membrane. *Proc Natl Acad Sci USA* 70:2853
70. Steinhoff HJ, Mollaaghababa R, Altenbach C, Hideg K, Krebs M, Khorana HG, Hubbell WL (1994) Time-resolved detection of structural changes during the photocycle of spin-labeled bacteriorhodopsin. *Science* 266:105–107
71. Váro G (1981) Dried oriented purple membrane samples. *Acta Biol Acad Sci Hung* 32:301
72. Shen Y, Safinya CR, Liang KS, Ruppert AF, Rothschild KJ (1993) Stabilization of the membrane protein bacteriorhodopsin to 140 °C in two-dimensional films. *Nature* 366:48
73. Koyama K, Yamaguchi N, Miyasaka T (1994) Antibody-mediated bacteriorhodopsin orientation for molecular device architectures. *Science* 265:762
74. Tans SJ, Dekker C (2000) Molecular transistors: potential modulations along carbon nanotubes. *Nature* 404:834
75. Bradley K, Cumings J, Star A, Gabriel J-CP, Gruner G (2003) Influence of mobile ions on nanotube based FET devices. *Nano Lett* 3:639
76. Freitag M, Radosavljevic M, Zhou Y, Johnson AT, Smith WF (2001) Controlled creation of a carbon nanotube diode by a scanned gate. *App Phys Lett* 79:3326
77. Bockrath M, Cobden DH, McEuen PL, Chopra NG, Zettl A, Thess A, Smalley RE (1997) Single-electron transport in ropes of carbon nanotubes. *Science* 275:1922
78. Javey A, Kim H, Brink M, Wang Q, Ural A, Guo J, McIntyre P, McEuen P, Lundstrom M, Dai H (2002) High-dielectrics for advanced carbon-nanotube transistors and logic gates. *Nat Mat* 1:241
79. Star A, Han T-R, Gabriel J-C P, Bradley K, Gruner G (2003) Interaction of aromatic compounds with carbon nanotubes: correlation to the Hammett parameter of the substituent and measured carbon nanotube FET response. *Nano Lett* 3:1421
80. Ehrenberg B, Berezin Y (1984) Surface potential on purple membranes and its sidedness studied by a resonance Raman dye probe. *Biophys J* 45:663
81. Cui Y, Wei Q, Park H, Lieber CM (2001) Nanowire nanosensors for highly sensitive and selective detection of biological and chemical species. *Science* 293:1289
82. Star A, Gabriel J-CP, Bradley K, Gruner G (2003) Electronic detection of specific protein binding using nanotube FET devices. *Nano Lett* 3:459–463